The Effect of Thermal Barrier Coated Piston Crown on Engine Characteristics

S.H. Chan and K.A. Khor

(Submitted 14 July 1998; in revised form 7 June 1999)

While there have been numerous research papers in recent years describing the theoretical benefits obtained from the use of ceramic components in reciprocating engines, the amount of literature that describes practical results is very limited. Although successes have been reported and ceramic components are now in service in production engines, mainly for reduced in-cylinder heat rejection, many researchers have experienced failures or a drop in engine performance. This article presents the work completed on a low heat rejection engine. Extensive experiments were conducted on a three-cylinder SI Daihatsu engine with piston crowns coated with a layer of ceramic, which consisted of yttria-stabilized zirconia (YSZ). Measurement and comparison of engine performance, in particular fuel consumption, were made before and after the application of YSZ coatings deposited onto the piston crowns. The details of the cylinder pressures during the combustion process were also investigated.

Keywords automotive tests, low heat rejection, partially stabilized ZrO_2, thermal barrier coatings, thermal engine tests, ZrO_2-8%Y_2O_3

1. Introduction

Thermal barrier coatings (TBCs) were used to simulate adiabatic engines with the intention not only for reduced in-cylinder heat rejection and thermal fatigue protection of underlying metallic surfaces, but also for possible reduction of engine emissions.[1–6] The application of TBCs reduces the heat transfer to the engine cooling jacket through the combustion chamber surfaces (which include the cylinder head, liner, and piston crown) and piston rings. The insulation of the combustion chamber with this coating, which is mainly ceramic based, influences the combustion process and hence the performance and exhaust emissions characteristics of the engines.[7–10] The former is easily understood from the first law of thermodynamics, although the reduced in-cylinder heat rejection may not favorably convert into a useful mechanical work but rather as an increased waste heat in the engine exhaust. The latter is extremely complicated because the increased air (or fuel-air mixture) temperature, due to the TBC (before the onset of combustion), could alter the ignition characteristic of the fuel-air mixture and its subsequent reaction mechanism, which are directly related to the exhaust emissions characteristics. Moreover, the thermophysical properties of the coated ceramic and its surface roughness and porous characteristic, either the pore size or porosity, have a direct influence on unburned or partially burned hydrocarbons through the surface quenching effect and their residence in the pores.[11,12]

The desire to increase thermal efficiency or reduce fuel consumption of engines makes it tempting to adopt higher compression ratios, in particular for diesel engines, and reduced in-cylinder heat rejection. Both of these factors lead to an increase in mechanical and thermal stresses. In particular, for the latter, durability concerns for the materials and components in the engine cylinders, which include piston, rings, liner, and cylinder head, limit the allowable in-cylinder temperatures. The application of thin TBCs to the surfaces of these components enhances high-temperature durability by reducing the heat transfer and lowering temperatures of the underlying metal.[13]

In this article, the main emphasis is placed on investigating the effect of a TBC on the engine fuel consumption with the support of detailed sampling of in-cylinder pressure. The optimization of the engine cycle and the exhaust waste heat recovery due to a possible increase in exhaust gas availability were not investigated in this study. Emission measurements of unburned hydrocarbons and carbon monoxide were also conducted in this study. The result of the latter is not included in this article because the difference before and after the application of a TBC is trivial, which is also within the resolution of the emission analyzer.

2. Zirconia Ceramics and TBCs

Zirconia ceramics have attracted much attention since their discovery, and the materials, which are very strong and tough at room temperature, can be made by control of the phases. Understanding of the phase transitions is crucial to appreciate the properties of zirconia ceramics. Zirconium dioxide (ZrO_2) has a monoclinic crystallographic structure at ambient temperatures. Upon raising the temperature, the oxide undergoes the phase transitions from monoclinic to tetragonal with a transitional temperature of 1170 °C. From tetragonal to cubic, the transition temperature is 2370 °C. At 2680 °C and above, the material melts. The transformation from tetragonal to monoclinic phase with decreasing temperature at approximately 1170 °C is quite disruptive and renders pure ZrO_2 unusable as a high-temperature structural ceramic. This disruption is caused by a 6.5% of volume expansion upon transformation from tetragonal to monoclinic phase, a change which could cause structural failure of any ceramic coating.

The ZrO_2 forms solid solutions with aliovalent oxides including CaO, MgO, and Y_2O_3 and the rare earth oxides. This can be

S.H. Chan and **K.A. Khor,** School of Mechanical and Production Engineering, Nanyang Technological University, Singapore 63 9798, Singapore. Contact e-mail: mkakhor@ntu.edu.sg.

achieved by intimate mixing of the powders, in this case the ZrO_2 and Y_2O_3; pressing to form a solid body; and sintering at a temperature sufficiently high to promote the interdiffusion of the cations. These solid solutions behave differently from pure ZrO_2 because the high-temperature phases, tetragonal and cubic, tend to stabilize at temperatures lower than 1170 and 2370 °C, respectively. Hence, doping of the previously mentioned aliovalent oxides serves as the stabilizing agent for the zirconia. In fact, with the addition of a sufficient fraction of stabilizer, the cubic phase could be stabilized at ambient temperatures. The addition of 9% mole fraction of yttria (Y_2O_3) or more to ZrO_2 will result in fully stabilized zirconia (FSZ), which has the cubic structure at all temperatures from ambient upward. Addition of 6% mole fraction of Y_2O_3 or less generates partially stabilized zirconia (PSZ), which consists of the cubic matrix with dispersed tetragonal or monoclinic precipitates, or both, depending on the temperature history. The selection of FSZ or PSZ for a TBC is important. When a crack forms in the coated material, the high stress concentration at the crack tip transforms the precipitates near the tip to the high volume monoclinic phase due to the pressure dependence of the tetragonal-monoclinic transformation. The increase in volume associated with this transformation reduces the stress at the crack tip and hence results in high strength and toughness. In this project, PSZ is adopted because of the previously mentioned advantage. The 8vol.%Y_2O_3, which is equivalent to 4.53%M fraction, was added to the ZrO_2 in this study. Before applying the TBC onto the piston crowns, a thickness of 600 μm of a new set of piston crowns was machined off. A bond coat of 150 μm and a yttria stabilized zirconia (YSZ) coat of 450 μm were then applied onto the piston crown by plasma spraying using a robot arm. The application of a TBC is only restricted to the piston crowns in this context because the surface constitutes a major part of the combustion chamber surfaces exposed to high-temperature gases. The authors posit that when thermal insulation is applied only to a certain part of the combustion chamber, it would surely increase the thermal loading of the others due to the increase in gas temperature. Extension of surface coating to other parts of the engine components is under exploration.

3. Experimental Setup

A fully instrumented SI Daihatsu (Daihatsu, Japan) engine was mounted on a computer-controlled engine dynamometer. Table 1 tabulates the specifications of the engine, while Fig. 1 shows the schematic of the overall arrangement of the engine test bed.

To appreciate the effect of a TBC on engine performance, in particular fuel consumption, obtaining engine indicator diagrams is necessary. A 10-mm water-cooled piezoeletric pressure transducer was used to measure the dynamic cylinder pressure. Unfortunately, the compact cylinder head design of the production

Table 1 Specifications of the engine

Type	Gasoline, four cycle
Cylinder number and arrangement	Three cylinder in-line, mounted transversely
Cylinder liner type	Integral with cylinder block
Total displacement, cm^3	993
Bore × stroke, mm	76 × 73
Compression ratio	9.5
Intake and exhaust layout	Cross-flow
Engine dimensions (length by width by height), mm	566 × 530 × 636
Engine weight, kg	92
Number of piston rings	Compression ring, 2 Oil ring, 1
Valve clearance [Hot], mm	Intake, 0.2 Exhaust, 0.2
Carburetor	Type, two barrel Throttle valve diameter, mm, 28, 32 Venturi diameter, mm, 18, 25

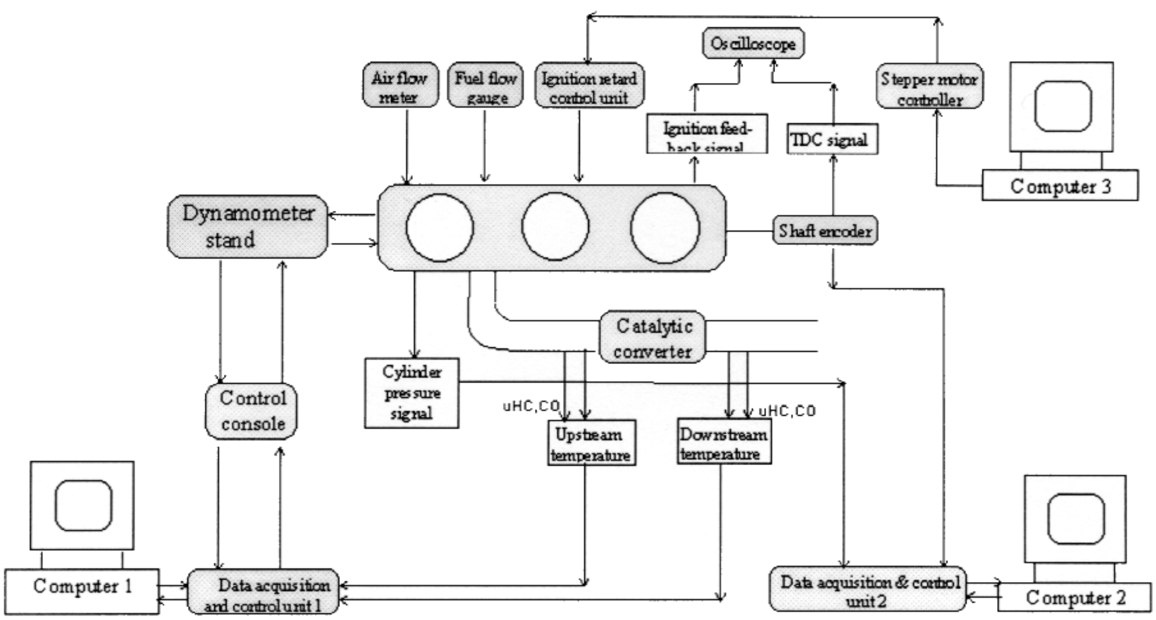

Fig. 1 Schematic of engine test bed arrangement

engine does not allow the transducer of this size to be directly mounted on it because no fill space is available for such installation. To fix the transducer, an adapter mounting was fabricated. To draw the pressurized gas out of the combustion chamber, a 2-mm through-hole was drilled into the third cylinder at the rear of the cylinder head (Fig. 2), the only place suitable for the mounting of the adapter and bypassing of the water jacket of the cylinder head.

In addition to pressure measurement, a. crank shaft encoder was used to trigger the acquisition of the pressure signal and also to provide crank positional information. The shaft encoder possessed a resolution of 0.1° crank angle (°CA); however, the data acquisition was set at a sampling rate of 0.2 °CA.

In this experiment, a nondispersive infrared (NDIR) analyzer and flame ionization detector (FID) measured concentrations of carbon monoxide and unburned hydrocarbons (uHCs), respectively.

The TBC was examined with scanning electron miscroscopy (SEM) after the tests had been conducted, and the chemical composition was analyzed with an energy dispersive x-ray (EDX) unit. Microhardness measurements were also taken on the polished cross section and surface.

4. Results and Discussion

Two sets of experiments were conducted and were named as baseline tests and TBC piston tests, respectively, which covered a wide range of engine operating spectra. In each set of tests, readings of engine speed, load torque, engine power, fuel consumption, exhaust gas temperature, gas emission concentrations, peak cylinder pressure, and so on, were taken for engine speeds from 1000 to 4000 rpm with an increment of 1000 rpm at 5, 25, 50, 75, and 90% relative to the maximum brake load of the baseline engine. To avoid the engine variability due to cyclic dispersion of firing, 200 readings at a sampling rate of 1 Hz were taken, after the engine had fully warmed k,up, for each operating condition, and the average value was used. Figures 3 to 6 show the results collectively.

Figure 3 shows the comparison of peak cylinder pressures between the baseline and TBC piston tests. The peak cylinder pressure was obtained from the sampling of cycle cylinder pressure, which was the ensemble average peak value of 500 cycles taken consecutively at a sampling rate of 0.2 °CA. Results show that the peak values were significantly increased in the TBC piston tests due to the low heat rejection at the cylinder walls. The increase in the temperature of the trapped gases in the combustion chamber, which caused the mean square velocity of the molecules and, hence, the pressure increase, can be explained by the kinetic theory. However, the increase in peak cylinder pressure is not just due to postignition low heat rejection; the better insulation actually altered the ignition characteristics, which had a great impact on the combustion process and increased peak cylinder pressure.

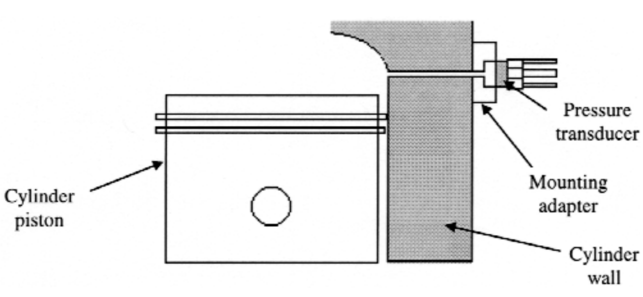

Fig. 2 External mounting of pressure transducer

Figure 4 compares the results obtained from both the baseline and TBC piston tests. In general, the TBC piston tests showed lower exhaust gas temperatures, which, combined with the results shown in Fig. 3, positively indicated that the performance of the engine would be improved. The increased peak cylinder pressure and reduced exhaust gas temperature in the TBC piston tests would mean that the net work output of the engine improved, which has been confirmed by good expansion of gases in the cylinder before the exhaust valves open.

Figure 5 shows the comparison of uHC concentrations between the baseline and TBC piston tests. For all cases, the uHC concentrations were higher in the TBC piston tests. The authors suspected that the increase in uHC concentrations in the engine tailpipe was likely due to the higher surface roughness and porosity of the ceramic coated piston crowns, which may have contributed to the porous quenching of the hydrocarbon fuel during the combustion. Though it is just a small amount in parts per million level, the physical characteristics of the material used have yet to be optimized for practical application.

In the emission measurements, the tailpipe uHC and CO concentrations were conducted. It was discovered that the CO did not vary much in either the baseline or TBC test. The variations were more or less within the resolution of the NDIR analyzer, which was ±0.1 vol.% concentration, whereas the resolution of the FID used was ± 1 ppm.

Figure 6 compares the brake specific fuel consumption between the baseline and TBC piston tests. Results show that, in general, the fuel consumption was lower in the TBC piston tests for the same operating condition, with an improvement of up to 6% at lower engine power. The self-optimized cycle efficiency due to the altered ignition characteristics in the TBC piston engine outnumbered the slightly reduced combustion efficiency with an overall improvement in thermal efficiency as a whole.

Figure 7 presents the pressure distribution in the engine cylinder, typically at 4,000 rpm varying load conditions, from −180 to 180 °CA, which covers the compression, ignition, combustion, and expansion of the charge. Analysis of the data point revealed that the ignition point of all TBC piston tests was slightly advanced relative to the baseline engine tests. The improved ignitability of the fuel-air mixture with reduced ignition delay caused more heat to be released before the top dead center of the cylinders. The combined effect of the continuing compression process and the increased heat release under improved thermal insulation of the piston crowns raised the maximum pressure. As the ignition advanced, there was an increase in thermal efficiency due to the increase in the effective expansion stoke that produced the positive work.

Figure 8 shows the SEM view of a polished cross section of the TBC layer after the tests. An oxide layer was observed between the YSZ topcoat and nickel-alloy bond coat. This was found to be essentially a mixture of Al_2O_3 and ZrO_2 with small amounts of NiO and Cr_2O_3 as well, which indicates that oxidation of aluminum, nickel, and chromium occurred during the

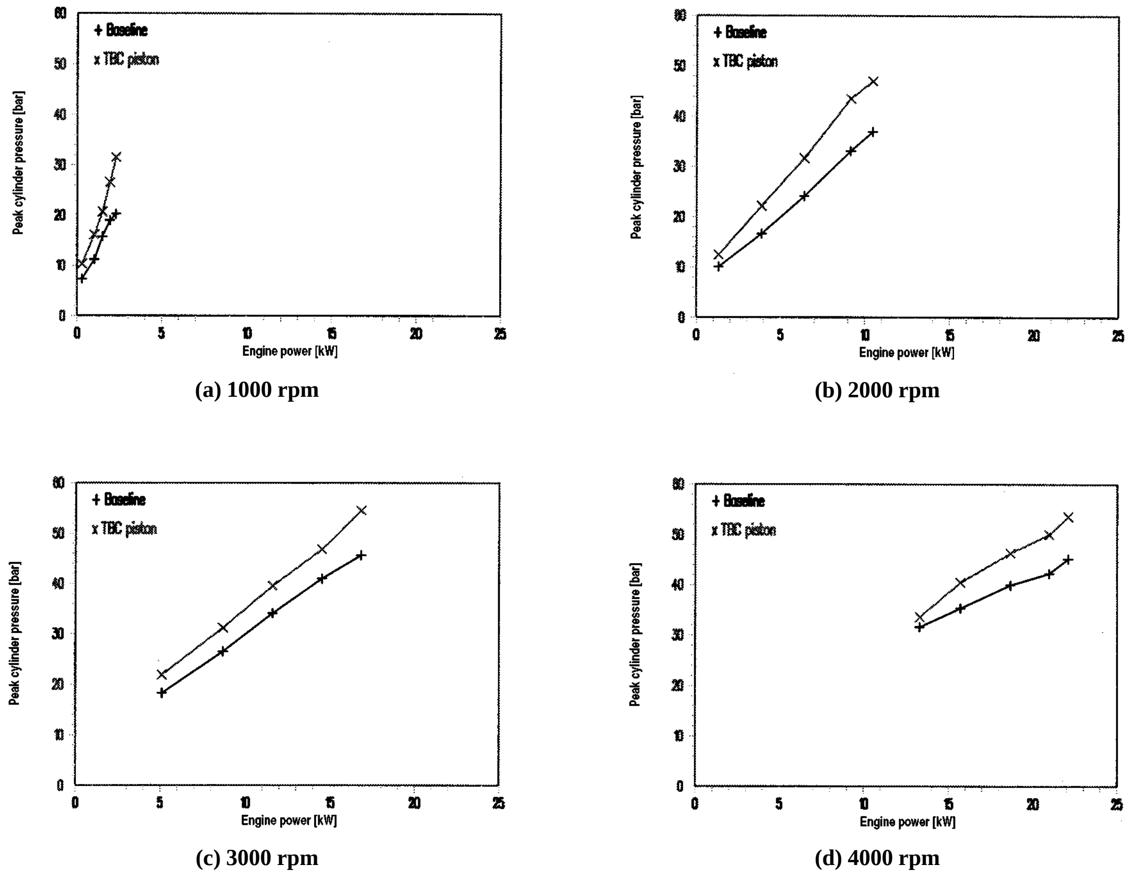

Fig. 3 **(a)** to **(d)** Comparison of peak cylinder pressures between baseline and TBC piston tests

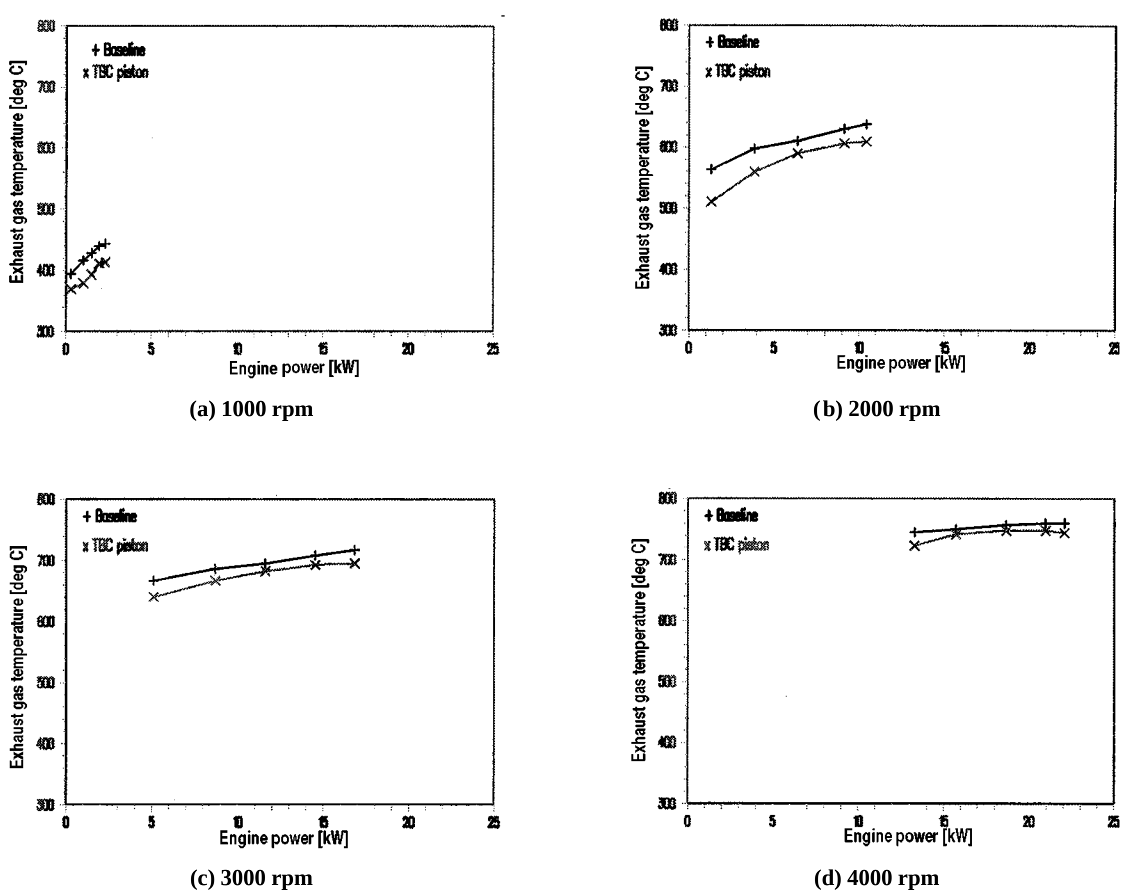

Fig. 4 **(a)** to **(d)** Comparison of exhaust gas temperatures between baseline and TBC piston tests

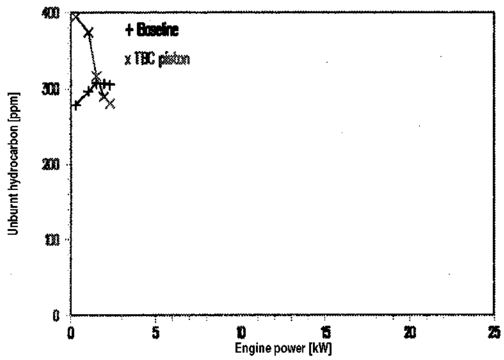

(a) 1000 rpm

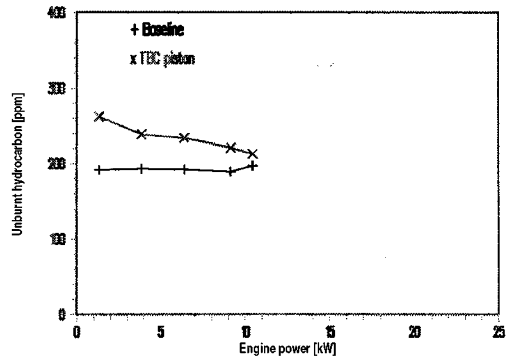

(b) 2000 rpm

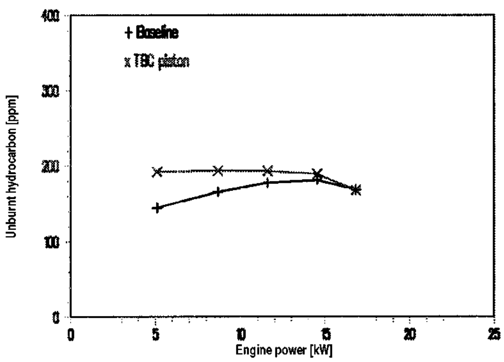

(c) 3000 rpm

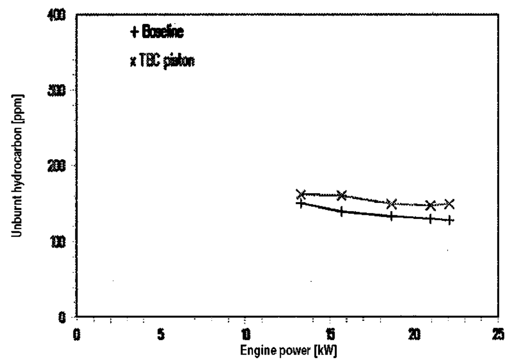

(d) 4000 rpm

Fig. 5 **(a)** to **(d)** Comparison of unburned hydrocarbon concentrations between baseline and TBC piston tests

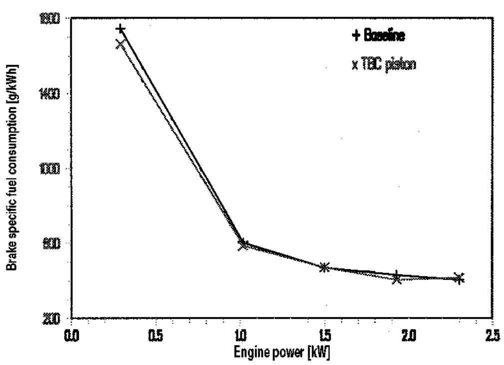

(a) 1000 rpm

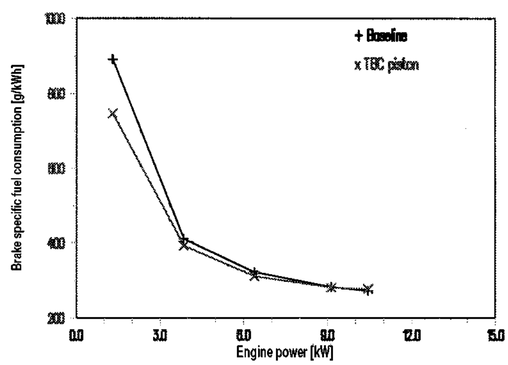

(b) 2000 rpm

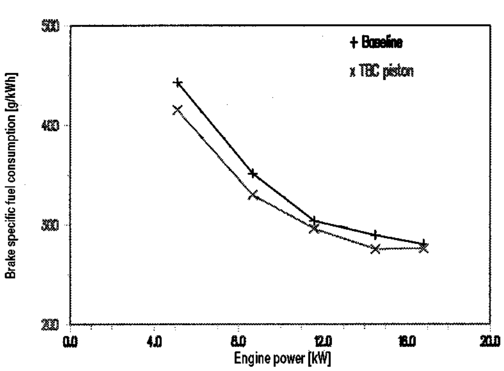

(c) 3000 rpm

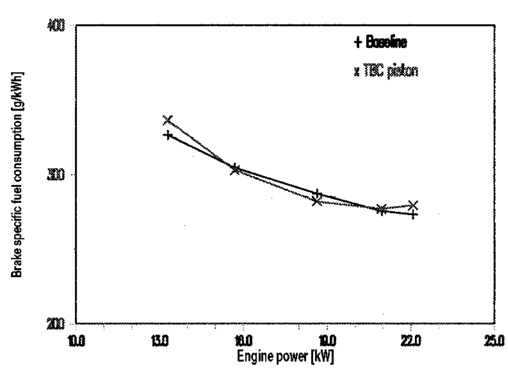

(d) 4000 rpm

Fig. 6 **(a)** to **(d)** Comparison of specific fuel consumption between baseline and TBC piston tests

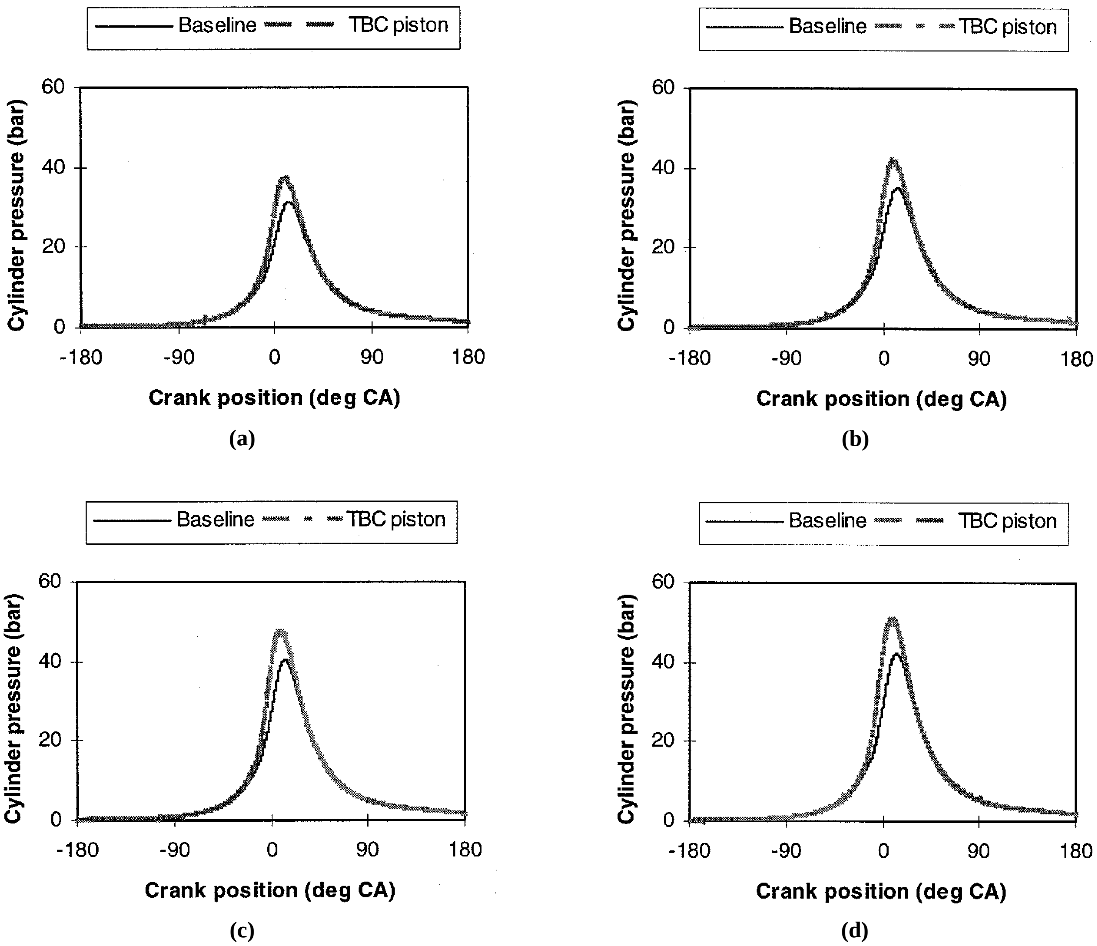

Fig. 7 Pressure distribution in the engine cylinder at 4,000 rpm varying load conditions. **(a)** 4,000 rpm/13.3 kW. **(b)** 4,000 rpm/15.7 kW. **(c)** 4,000 rpm/21.0 kW. **(d)** 4,000 rpm/22.1 kW

tests. The overall microhardness value of the YSZ top layer obtained was 417 ± 26 HV. This value is typical of most as-sprayed TBC layers, indicating that the microhardness values of YSZ were not affected by the test conditions.

5. Conclusions

The following conclusions can be drawn.

- The TBC, using YSZ, applied to the combustion chamber of the internal combustion engine showed some improvement in fuel economy with a maximum of up to 6% at low engine power.
- The peak cylinder pressures were increased by a magnitude of eight to ten bars in the TBC piston engine, in particular at high engine power outputs, though the exhaust gas temperatures were generally lower, indicating good gas expansion in the power stroke.
- The unburned hydrocarbon concentrations were increased most seriously at low engine speed and/or low engine power output with a TBC piston engine. The authors suspected that this could be due to the porous quenching effect of the rough TBC piston crowns, where oxidation of hydrocarbons was unable to be achieved by the combustion air.
- Sampling of cylinder pressures in the cylinders showed that the ignition point of the TBC piston engine advanced slightly relative to the baseline engine, indicating the improvement in ignitability and heat release before the top dead center, which caused the peak cylinder pressure to raise.
- While there was no apparent drop in microhardness, a layer of mixed oxide formed between the YSZ top coat and nickel alloy bond coat, indicating that oxidation of the aluminum in the bond coat occurred during the engine tests.

References

1. C.C.J. French: “Ceramics in Reciprocating Internal Combustion Engines,” SAE Paper No. 841135, SAE, Warrendale, PA, 1984.
2. C.H. Moore and J.L. Hoehne: “Combustion Chamber Insulation Effect on the Performance of a Low Heat Rejection Cummins V-903 Engine,” SAE Paper No. 860317, SAE, Warrendale, PA, 1986.
3. R.A. Churchill, J.E. Smith, N.N. Clark, and R.A. Turton: “Low Heat Rejection Engines—A Concept Review,” SAE Paper No. 880014, SAE, Warrendale, PA, 1988.

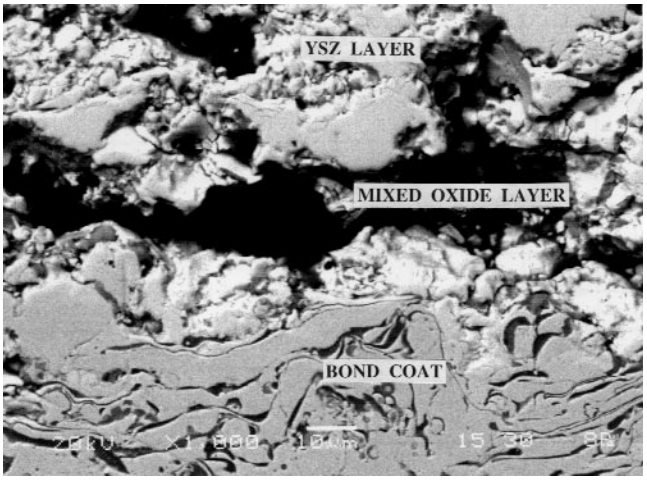

(a)

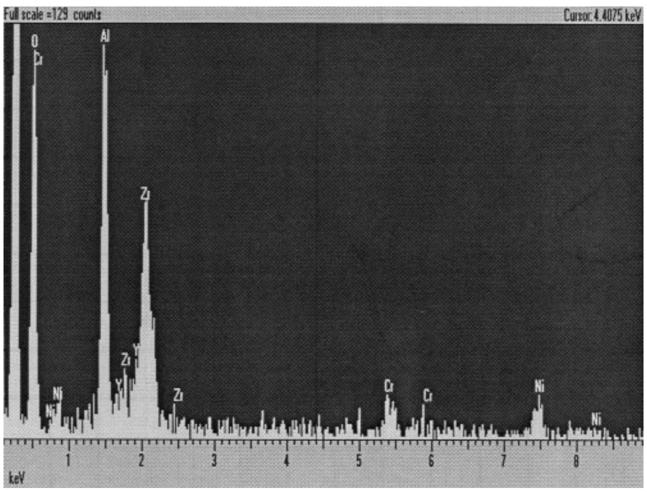

(b)

Fig. 8 **(a)** SEM view of polished cross section showing the oxide layer between the top coat (YSZ) and the bond coat. **(b)** The EDX spectrum of the oxide layer indicating a mixture of aluminum and zirconium oxides

4. D.H. Harris and J. Lutz: "Thermal Barrier Coatings—Technology for Diesel Engines," SAE Paper No. 880437, SAE, Warrendale, PA, 1988.
5. C.S. Reddy, N. Domingo, and R.L. Graves: "Low Heat Rejection Engine Research Status: Where Do We Go from Here?" SAE Paper No. 900620, SAE, Warrendale, PA, 1990.
6. T.M. Yonushonis: *J. Thermal Spray Technol.*, 1997, vol. 6 (1), pp. 50-56.
7. V. Sudhakar: "Performance Analysis of Adiabatic Engine," SAE Paper No. 840431, SAE, Warrendale, PA, 1984.
8. D. Assanis, K. Wiese, E. Schwarz, and W. Bryzik: "The Effects of Ceramic Coatings on Diesel Engine Performance and Exhaust Emissions," SAE Paper No. 910460, SAE, Warrendale, PA, 1991.
9. S. Kimura, Y. Matsui, and T. Itoh: "Effects of Combustion Chamber Insulation on the Heat Rejection and Thermal Efficiency of Diesel Engines," SAE Paper No. 920543, SAE, Warrendale, PA, 1992.
10. E. Scharwz, M. Reid, W. Bryzik, and E. Danielson: "Combustion and Performance Characteristics of a Low Heat Rejection Engine," SAE Paper No. 930988, SAE, Warrendale, PA, 1993.
11. R.M. Frank and J.B. Heywood: "The Effect of Piston Temperature on Hydrocarbon Emissions from a Spark-Ignited Direct-Injection Engine," SAE Paper No. 910558, SAE, Warrendale, PA, 1991.
12. J.T. Wentworth: "More on Origins of Exhaust Hydrocarbons—Effects of Zero Oil Consumption, Deposit Location, and Surface Roughness," SAE Paper No. 920939, SAE, Warrendale, PA, 1992.
13. M.H. Haselkorn: *J. Thermal Spray Technol.*, 1995, vol. 4.